IEEE Photonics Journal
An IEEE Photonics Society Publication

Open Access

Near-Infrared Reflectivity of Superconducting FeSe Thin Films

Volume 11, Number 3, June 2019

Yanmin Zhang
Wen Xu
Zhongpei Feng
Zefeng Lin
Kui Jin
Jie Zhang
Shun Zhou
Zhaojun Liu
Chen Guan
Tiandi Chen
Junqi Wang
Lan Ding
Sasa Zhang

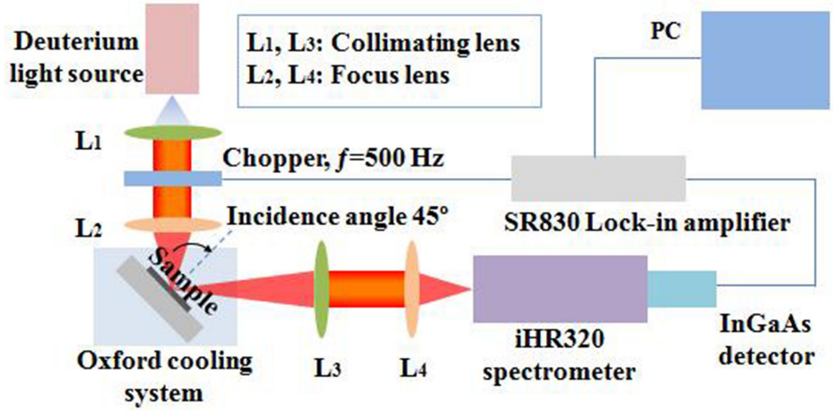

DOI: 10.1109/JPHOT.2019.2910668
1943-0655 © 2019 IEEE

Near-Infrared Reflectivity of Superconducting FeSe Thin Films

Yanmin Zhang,[1] Wen Xu,[2,3] Zhongpei Feng,[4] Zefeng Lin,[4] Kui Jin,[4] Jie Zhang,[3] Shun Zhou,[3] Zhaojun Liu,[1] Chen Guan,[1] Tiandi Chen,[1] Junqi Wang,[1] Lan Ding,[3] and Sasa Zhang[1]

[1]School of Information Science and Engineering, Shandong University, Jinan 250100, China
[2]Key Laboratory of Materials Physics, Institute of Solid State Physics, Chinese Academy of Sciences, Hefei 230031, China
[3]School of Physics and Astronomy, Key Laboratory of Quantum Information of Yunnan Province, Yunnan University, Kunming 650091, China
[4]National Laboratory for Superconductivity, Institute of Physics, Chinese Academy of Sciences, Beijing 100190, China

DOI:10.1109/JPHOT.2019.2910668

Manuscript received February 15, 2019; revised April 5, 2019; accepted April 8, 2019. Date of publication April 15, 2019; date of current version May 1, 2019. This work was supported in part by the National Key Basic Research Program of China (2015CB921003); in part by the Center of Science and Technology of Hefei Academy of Science (2016FXZY002); in part by the National Natural Science Foundation of China (11574319, 11364045, 11764045, and U1832153); and in part by the Department of Science and Technology of Yunnan Province (2016FC001). Corresponding authors: Wen Xu, Lan Ding, and Sasa Zhang (e-mail: wenxu_issp@aliyun.com; dinglan@ynu.edu.cn; sasazhang@sdu.edu.cn).

Abstract: We present an investigation on the intrinsic optical properties of superconducting FeSe thin films deposited on CaF_2 substrates. It is found that the samples respond strongly to the near-infrared (NIR) irradiation in different temperature regimes. Thus, we are able to measure the optical reflectivity of the in-plane (ab-plane) thin films from room temperature to 5 K. A critical behavior near the superconducting transition temperature (T_c∼10 K) can be observed optically in the temperature-dependent reflectivity spectrum. We carry out the Kramers–Kronig analysis of the experimental data and discuss the basic optical properties of superconducting FeSe thin films in different structural phases above and below the transition temperature T_s∼100 K. By fitting experimental data with the Drude–Smith and Drude–Lorentz formulas, we obtain the key sample parameters such as the electronic relaxation time and dc conductivity. The interesting and important findings obtained from this study not only shed new light on the pairing mechanism in FeSe but also demonstrate that the NIR reflection experiment is a powerful and convenient optical technique for contactless characterization and investigation of superconducting thin film materials.

Index Terms: Infrared, reflection, thin films, optical properties, spectrum analysis

1. Introduction

Since the discovery of high-T_c superconductivity in iron-based superconductors (FeSCs) in 2008 [1], considerable experimental and theoretical studies have been devoted to explore their characteristic features such as electronic structure, transport properties, superconductivity, structural and electronic phase transitions, etc. [2], [3]. FeSe is a typical FeSC which can be applied for understanding the microscopic mechanism of the superconductivity because of its simple crystal structure [4]. In recent years, the related research attention has been focused on the electronic structure and

TABLE 1
The Detailed Parameters for Samples

	FeSe	Thickness	T_c(zero)	T_c(onset)
Sample A	1:1	160 nm	9.55 K	11.25 K
Sample B	1:1	160 nm	9.26 K	11.53 K

superconductivity in FeSe thin films with a single unit cell deposited on $SrTiO_3$ and CaF_2 substrates [5]–[11]. Very recently, we have fabricated high quality FeSe single crystal thin films via epitaxial growth on the CaF_2 substrates and have conducted the investigation of the corresponding electronic structure, superconductivity, transport properties, and magnetism of these thin films [12], [13]. In particular, because we have obtained the high quality and relatively large-size single crystal FeSe thin film samples, it now becomes possible to examine the basic physical properties of FeSe thin films via optical measurements. As a matter of fact, the optical properties of FeSe thin films or bulk materials have been measured via conventional optical experiments [14]–[17]. Nakajima *et al.* [16] reported the optical properties of FeSe film on CaF_2 substrate. They found an anomalous behavior of the optical phonon mode below structural phase transition temperature T_s at 40.16 μm which implies the orbital origin of the structural transition [16]. They also observed two interband transitions at about 2 μm and 5 μm [16], but did not report the superconducting transition below 2 μm [14], [16]. It is known that the optical measurement is a powerful, effective and non-invasive experimental approach in studying the electronic systems and in obtaining the key sample and material parameters of an electronic system [18]–[21]. In contrast to electric transport measurement on a field effect transistor (FET) or Hall bar device, the contact electrodes on the sample are often not required in optical experiments. Moreover, through examining the temperature dependence of the optical spectroscopy for superconducting thin films, one can investigate optically the features of the coexistence of the superconducting and other electronic and structural phases [22], [23] and examine the electronic and optical properties of FeSe in different temperature regimes.

In this work, we present an optical spectroscopic study on the in-plane properties of FeSe thin films on CaF_2 substrates from 5 to 300 K through near-infrared (NIR) reflection experiments. The present study is focused on the optical properties of FeSe thin films in both the normal and superconducting states. We intend to examine the temperature-induced metal-superconductor transition (MST) and the dependence of the real and imaginary parts of the optical conductivity upon NIR radiation wavelength. We analyze the data using Drude-Lorentz and Drude-Smith model at selected temperatures both below and above the structural phase transition temperature T_s. Meanwhile, the corresponding optical parameters can be obtained.

2. Experimental Details

In this study, high-quality FeSe single crystal thin films are prepared on CaF_2 substrates by pulsed laser deposition (PLD) technique. The details of the sample fabrication and characterization for the FeSe thin films can be found in previous reports [13], [24]. In the present study, two FeSe films (Samples A and B) with slightly different T_c are studied and their key material parameters are listed in Table 1. The size of these CaF_2 substrates are 5 mm $\times$ 5 mm $\times$ 0.5 mm and the thickness of FeSe epitaxial thin films is about 160 nm. The X-ray diffraction (XRD) results are shown in Fig. 1 (left panel), where only (00l) peaks can be observed, indicating that these FeSe films are in single crystal phase. Hence, the FeSe thin film samples used in this study are with good lattice orientations and high single crystal quality. The middle panel of Fig. 1 shows the surface morphologies of these FeSe thin films by scanning electron microscope (SEM). Here, the precipitates observed are the common characteristic of the samples prepared via PLD method. Moreover, the stoichiometric Fe:Se ratio of 1:1 for these samples are confirmed by energy dispersive spectroscopy (EDS). The results from elemental composition of the EDS spectra for these FeSe films are also shown in Fig. 1

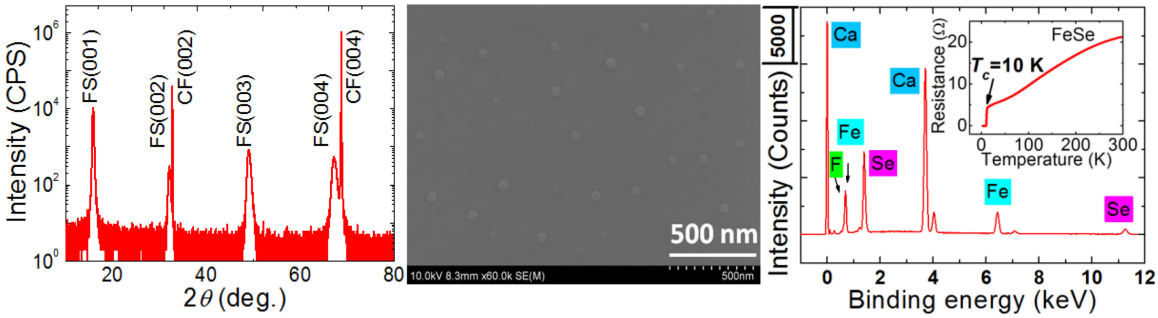

Fig. 1. X-ray diffraction pattern (left panel) of an FeSe thin film grown on <001> CaF_2 substrate. SEM image (middle panel) and the corresponding EDS spectrum (right panel) for the top surface of the FeSe sample. The inset (in the right panel) shows the temperature dependence of resistance for superconducting FeSe thin film.

(right panel). The corresponding φ-scan and ω-scan [24] along with the STEM [25] results for these FeSe thin films have been documented previously in the literature.

We then carry out the measurement of longitudinal resistivity (ρ_{xx}) and Hall coefficient (R_H) from 2 to 300 K [25]. We find that the superconducting transition temperature for FeSe thin film is $T_c \sim 10$ K from the temperature dependence of resistance shown in Fig. 1 (right panel inset). In the temperature regime of 20 K $< T <$ 90 K, the temperature dependence of electron mobility (μ_e) and hole mobility (μ_h) for FeSe thin film samples with different T_c temperatures can be obtained by the two-carrier model [25]. When the temperature T is below 20 K or larger than about 90 K, this model cannot fit well to experimental data because of the superconducting fluctuations and the structural transition, respectively [25], [26]. In the low temperatures from 10 to 20 K, the dominant contribution carriers to affect the transport properties are holes [27]. In this temperature regime R_H is induced by holes alone in the sample so that $R_H = 1/(n_h e)$, where n_h is the hole density which is about 2.45×10^{20} cm^{-3} at 20 K [25]. The hole mobility obtained from electrical transport measurement is about $\mu_h = 100$ cm^2/(V s) at 20 K [25]. Considering that the effective mass for holes in FeSe is $m^* \sim 1.3\ m_0$ [27] with m_0 being the rest electron mass, we find that the electronic relaxation time $\tau = \mu m^*/e$ for FeSe thin film in metallic phase is of the order of 50 fs at 20 K, which is in line with the result obtained from corresponding THz transmission measurement [27].

It is known that the superconductivity and electric conductance depend strongly on carrier concentration [28], [29] and electronic relaxation time induced by scattering centers. When the condition $\omega\tau \sim 1$ is satisfied, with ω being the radiation frequency, the response of electrons in an electronic system to optical irradiation can be observed so that the optical coefficients such as optical transmission and reflection along with corresponding optical conductivity are the functional form of the radiation frequency. The electronic relaxation time $\tau \sim 50$ fs, measured via transport experiment for FeSe thin films, implies that the near-infrared (NIR) optical experiment can be applied for the investigation of optical properties of FeSe single crystals. For our samples, the thickness of the CaF_2 substrate is about 0.5 mm, which is much larger than NIR wavelength. As a result, the strong absorption of the incident NIR light by the substrate can occur. Therefore, the NIR reflection experiment is a good option for studying the optical property of the FeSe thin film on such a dielectric substrate. Furthermore, because the thickness of the FeSe thin film is about 160 nm, which is far less than the NIR light wavelength, the reflection pattern induced by thin-film interference effect can be avoided in the measurements.

In our custom-built experimental setup, the optical reflection (OR) spectrum measurements are carried out in the NIR bandwidths with the spectral range from 1.1 to 1.9 μm in wavelength. The schematic diagram of the NIR measurement is shown in Fig. 2. In the reflection experiments, the standard deuterium lamp is employed as a broadband NIR incident light source. The incident and emergent light beams are both with an angle 45° to the FeSe sample surface. In this configuration, the incident light field can couple with the electrons in the ab-plane for FeSe thin films and, thus, the

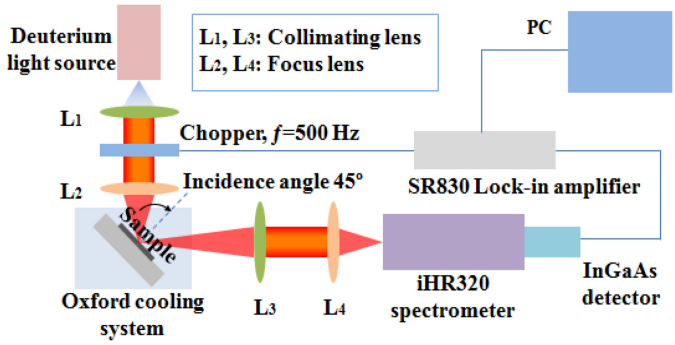

Fig. 2. Schematic diagram of the NIR reflection measurement for FeSe thin films. Here L_1 and L_3 are collimating lens and L_2 and L_4 are light focusing lens.

OR spectrum can carry the information about how electrons in the sample respond to the applied radiation field. In Fig. 2, L_1 and L_3 are collimating lens and L_2 and L_4 are focus lens. The OR spectrum is recorded using an imaging spectrometer (iHR320 HORIBA Jobin Yvon, USA) and the InGaAs photodetector is used for the detection of the NIR light beams in 1.1–1.9 μm wavelength regime. In the experiments, the results of NIR reflection spectra from Cu mirror are applied as reference. Because both samples and CaF_2 substrates are with relatively higher transmittance in the NIR bandwidth, the results of the measurement on Cu mirror can reflect the main profile of the radiation light source. The frequency and temperature dependence of reflectivity spectrum for CaF_2 below 16.7 μm is negligible [16], [30], since CaF_2 has the stable and good transmittance performance for a broad wavelength range of 0.125–10 μm [31]. The depth of penetration of NIR radiance is about several tens of nanometers for metal materials and, thus, the NIR reflectivity from CaF_2 substrate can be negligible. As a result, the reflectance spectrum measured in the experiment contains mainly the intrinsic behavior of the FeSe films. We measure the reflection spectra for both FeSe thin films in (001)-orientation and the Cu mirror as a function of temperature, where the variation of temperature is achieved in a liquid-helium closed cycle cooling system (Oxford, UK). For Sample A (B), the measurements are undertaken in temperature range from 5 to 300 K (40 K). It should be noted that because the intensity of NIR light reflection from Cu mirror depends on temperature, we measure the temperature dependence of the NIR reflection from Cu mirror upon temperature in order to obtain more accurate data for reflectivity of the FeSe thin film at a given temperature.

3. Results

By definition, the optical reflectivity of a sample at a given temperature is the ratio of the measured light reflection intensity of the sample (FeSe thin film plus substrate) and the reference (Cu mirror) at the same temperature. The corresponding NIR reflectivity spectra for Sample A at different temperatures at 5, 10, 20, 50, 100, 150, 200, 250, and 300 K are shown in Fig. 3 (left panel). The dependence of optical reflection upon temperature is a consequence of the fact that the dc conductivity and electronic relaxation time in an FeSe thin film depend on temperature. As we can see from the left panel of Fig. 3 that within radiation wavelength regime 1.1–1.9 μm, the reflectivity for a FeSe thin film first increases (5–10 K) then decreases (10–300 K) monotonically with increasing temperature, and the intensity of the reflectivity depends rather weakly on radiation wavelength at a given temperature, especially at high temperatures. It should be noticed that the small peaks at about 1347 and 1556 nm in Fig. 3 (left panel) are the characteristic lines of the deuterium lamp.

To study the characteristics of temperature dependence of the reflectivity, in right panel in Fig. 3 we plot the optical reflectivity for FeSe samples A and B (inset) as a function of temperature at different radiation wavelengths. A notable change of the NIR reflectivity can be observed at about 10 K for radiation wavelength from 1.1 to1.9 μm. The peak position at about 10 K corresponds

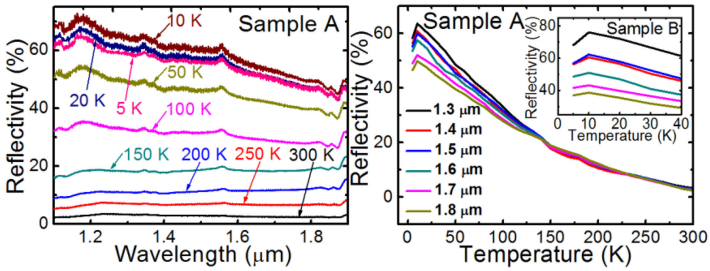

Fig. 3. NIR reflectivity spectra for Sample A (left panel) at different temperatures as indicated. NIR reflectivity for Sample A (right panel) as a function of temperature at different radiation wavelengths 1.3, 1.4, 1.5, 1.6, 1.7 and 1.8 μm as indicated. A notable change of the NIR reflectivity can be observed at about 10 K, and the same change can be observed in Sample B (right panel inset).

to superconducting transition temperature T_c for Sample A and Sample B. We notice that in the measurement, the accuracy of the temperature control is of the order of 1 K. Thus, a roughly the same T_c is measured for both Sample A and Sample B. We find that the same $T_c \sim 10$ K can be measured at different radiation wavelengths from 1.1 to 1.9 μm, which implies that the NIR experiment using the standard deuterium lamp as a broadband light source does not affect the electronic structure of the FeSe thin film material.

For optical study of an electronic system, optical conductivity is the key physical quantity from which we can obtain other optical parameters such as transmission, absorption, and reflection coefficients via basic physics laws. The complex optical conductivity can be written as $\sigma(\omega) = \sigma_1(\omega) + i\sigma_2(\omega)$ with $\sigma_1(\omega)$ and $\sigma_2(\omega)$ being the real part and imaginary part respectively. In optical reflection experiment, the optical reflectivity: $R(\omega) = (N-1)/(N+1)$ where $N = n(\omega) + i\kappa(\omega)$ with $n(\omega)$ and $\kappa(\omega)$ being respectively the refractive index and extinction coefficient. Thus, the real and imaginary parts of the optical conductivity are given as

$$\sigma_1(\omega) = \omega\varepsilon_0 \left[2n(\omega)\kappa(\omega)\right], \tag{1}$$

and

$$\sigma_2(\omega) = \omega\varepsilon_0 \left[1 - n^2(\omega)\kappa^2(\omega)\right], \tag{2}$$

where ε_0 is the permittivity of the free space. In the present experiment we are unable to measure directly the imaginary part of the reflectivity. However, we can get this quantity via standard Kramers-Kronig (K-K) transformation of the experimental data for $R(\omega)$. The phase angle $\theta(\omega)$ of the optical reflectivity can be evaluated via K-K transformation, $\theta(\omega) = -\frac{\omega}{\pi} P\left[\int_0^\infty \frac{\ln R(s)}{s^2-\omega^2} ds\right]$. In the present study, we take the Hagen-Rubens relation: $R(\omega) = 1\text{-}A\omega^{1/2}$ for the low frequency (below 2 μm) extrapolation and $R(\omega) \sim \omega^{-4}$ for high frequency (above 1 μm) extrapolation. It should be noted that for a FeSe thin film the NIR irradiation can result in interband electron transition [17], [32] because the NIR photon energy is larger than electronic band gap of the FeSe material. Using the reflectivity obtained experimentally and the phase angle obtained via K-K transformation we can get respectively the refractive index $n(\omega) = \frac{1-R(\omega)}{1-2\sqrt{R(\omega)}\cos\theta(\omega)+R(\omega)}$ and the extinction coefficient $\kappa(\omega) = \frac{2\sqrt{R(\omega)}\sin\theta(\omega)}{1-2\sqrt{R(\omega)}\cos\theta(\omega)+R(\omega)}$.

In Fig. 4(a) and (b) we show the NIR spectra for respectively the real $\sigma_1(\omega)$ and imaginary $\sigma_2(\omega)$ parts of the optical conductivity measured at different temperatures. From $\sigma_1(\omega)$ shown in Fig. 4(a), we see that in NIR regime the real part of the optical conductivity for FeSe does not decrease monotonously with increasing ω at different temperatures. From $\sigma_2(\omega)$ shown in Fig. 4(b), we find that the imaginary part of the optical conductivity for FeSe can become negative in NIR bandwidth. These results imply that the optical conductivity for FeSe cannot be described rightly by the standard Durde formula which gives that $\sigma_1(\omega)$ should decrease with increasing ω and $\sigma_2(\omega)$ should always be positive. In superconducting phase ($T < 10$ K), the optical conductivity in NIR bandwidth is mainly induced by the correlation effect of FeSe superconductor in the presence of the Hund's coupling of Fe 3*d* orbitals [33], [34]. From $\sigma_2(\omega)$ shown in Fig. 4(b), we notice that when $T > 100$ K the

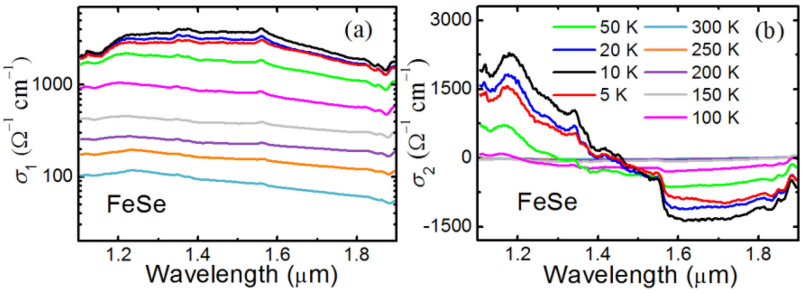

Fig. 4. The spectra for real $\sigma_1(\omega)$, in (a), and imaginary $\sigma_2(\omega)$, in (b), parts of optical conductivity in an FeSe thin film at different temperatures as indicated.

imaginary part of the optical conductivity depends very weakly on temperature, whereas a strong dependence of $\sigma_2(\omega)$ upon temperature can be observed when $T \leq 100$ K. Furthermore, when $T < 100$ K, $\sigma_2(\omega)$ can even change the sign with varying ω. It is known that the upper Se-Fe-Se angle or two Fe-Fe distances can be altered across $T_s \sim 90$ K [35], which mainly affects the Fe 3*d* orbital [16] and results in a tetragonal to orthorhombic structural phase transition [35]. Therefore, in different structural phases the electronic mobility or dc conductivity should be different in FeSe where the Hund's coupling between itinerant electrons and localized electrons plays an important role in determining the electronic and optical properties of FeSe [33].

FeSe is an electronic material which can have phase-transition induced by temperature [35], radiation field [16] and other experimental conditions. It is interesting to note that in FeSe, a tetragonal to orthorhombic structural phase transition occurs at about $T_s \sim 90$ K [35]. Different electronic phases correspond to different mechanisms of the electronic transition accompanied by the absorption of NIR photons. Thus optical conductivity in different phases of FeSe can be achieved via different mechanisms. As a result, different theoretical models for optical conductivity have to be applied for the examination of the optical properties in the sample. Usually, in conventional metals and semiconductors, optical conductivity can often be described simply using, e.g., the Drude formula: $\sigma(\omega) = \sigma_0/(1\text{-}i\omega\tau)$, where $\sigma_0 = N_e e^2\tau/m^*$ is the dc conductivity with N_e being the carrier density, m^* the effective electron mass and τ the electronic momentum relaxation time. However, it is known that in infrared charge dynamics, the iron-based superconductors have pronounced bad-metal characteristics [36]. We find that when temperature is below about 100 K, the complex conductivity obtained experimentally can be well described by the Drude-Lorentz formula [37],

$$\sigma(\omega) = \sigma_0 \frac{\omega\tau}{i(\omega_0^2 - \omega^2)\tau^2 + \omega\tau}. \tag{3}$$

Here ω_0 is a resonance frequency of a Lorentz oscillator. When the temperature is above 100 K, the complex conductivity obtained experimentally can be fitted nicely to a modified Drude formula or the Drude-Smith formula via [38],

$$\sigma(\omega) = \frac{\sigma_0}{1 - i\omega\tau}\left[1 + \sum_{n=1}^{\infty} \frac{c_n}{(1 - i\omega\tau)^n}\right]. \tag{4}$$

Here a coefficient $c_n = [-1, 0]$ describes the fraction of original velocity for an electron after the *n*th collision event, which reflects the effect of electronic localization. For a nonzero c_n or in the presence of electronic localization effect, the optical conductivity can increase with $\omega\tau$ [38]. We find that when taking $n = 1$, i.e., $\sigma(\omega) = \sigma_0/(1 - i\omega\tau)[1+c/(1 - i\omega\tau)]$ with $c = c_1$, good fitting between experimental data and Drude-Smith formula can be achieved.

In Fig. 5, we show the results of fitting of the real and imaginary parts of the optical conductivity obtained from K-K transformation of the experimental data with the theoretical formulas. As we can see, the experimental data fit well to the Drude-Lorentz formula (Drude-Smith formula) at $T = 50$ K (150 K) as shown in Fig. 5(a) (Fig. 5(b)). We find that when $T \leq 100$ K ($T > 100$ K), the good fitting

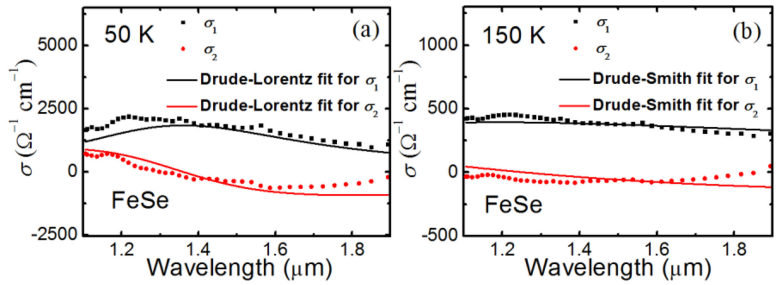

Fig. 5. The fitting of the experimental data for the real (black dots) and imaginary (red dots) parts of the optical conductivity with the Drude-Lorentz formula at 50 K in (a) (black and red curves) and with the Drude-Smith formula at 150 K in (b) (black and red curves).

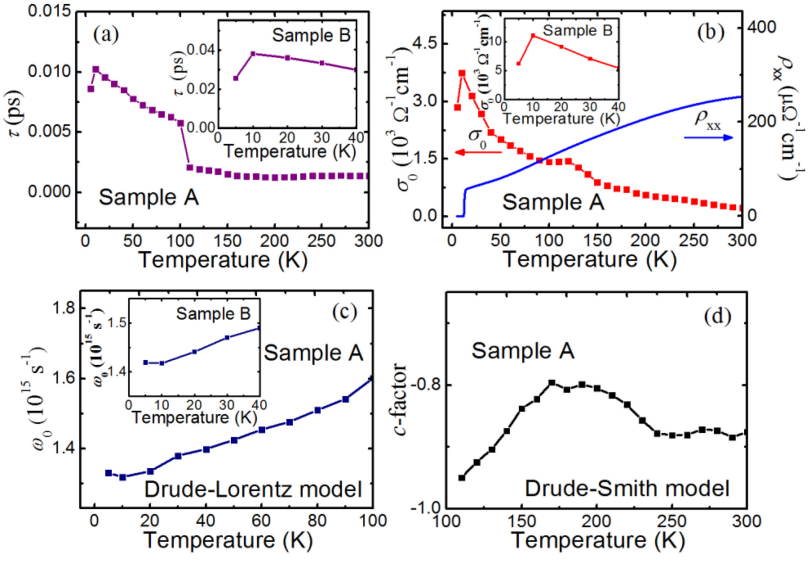

Fig. 6. Temperature dependences of the relaxation time τ in (a) and dc conductivity σ_0 in (b) for FeSe thin film sample A obtained by the Drude-Lorentz fitting ($T \leq 100$ K) and the Drude-Smith fitting ($T > 100$ K) and the corresponding results for sample B (insets) around T_c temperature. Here we also show the results of the dc resistivity obtained from electric transport measurement (blue curve in (b)). The Lorentz oscillation frequency ω_0 and the electronic localization factor c for FeSe thin film sample A and B (inset) are shown, respectively, in (c) and (d) as a function of temperature in different temperature regimes.

of the experimental results and the theoretical formula can be achieved by using Drude-Lorentz formula (Drude-Smith formula). This finding confirms that the FeSe samples undergoes the phase transition around 100 K.

Through fitting of the real and imaginary parts of the optical conductivity obtained experimentally with theoretical formula, we are able to obtain optically the key material parameters such as the electronic relaxation time τ, the electron density N_e, and the Lorentz frequency ω_0 or electronic localization factor c. In Fig. 6(a) and (b) we show respectively the electronic relaxation time τ and the dc conductivity $\sigma_0 \sim N_e e^2 \tau / m^*$ as a function of temperature for FeSe thin film samples. In normal phase for FeSe, $T > 10$ K, τ decreases with increasing temperature (see Fig. 6(a)), similar to a normal metal or semiconductor due to electron-phonon scattering whose coupling strength is proportional to phonon occupation number $N_Q = [\exp(\hbar\omega_Q / k_B T) - 1]^{-1}$, with $\hbar\omega_Q$ being the phonon frequency. This leads to a decrease in σ_0 with increasing temperature in normal state, in line with the dc resistivity ρ_{xx} obtained from electric transport measurement (blue curve in Fig. 6(b)). Fig. 6(c) and (d) show the temperature dependence of the Lorentz frequency ω_0 and electronic localization factor

c, respectively, in different temperature regimes. ω_0 increases with temperature for samples A and B below 100 K, which implies that the elementary electronic excitation increases with temperature in FeSe. Above 100 K, the electronic localization factor c depends rather weakly on temperature but with a relatively big value at about -0.9, which implies a strong electronic localization effect in FeSe in high-temperature region.

The results obtained from electric transport measurement on FeSe thin films [12], [13], [25] indicate that in normal state, the dc resistivity ρ_{xx} of the sample increases monotonically with temperature from T_c up to room temperature in Fig. 6(b). This suggests that the electrons in a FeSe thin film are in a metallic state when $T > T_c$. In a metallic phase, the optical absorption, transmission and reflection all occur simultaneously in a FeSe thin film. The absorptivity A, the transmissivity T_o, and the reflectivity R should satisfy the energy conservation law: $A + T_o + R = 1$. Normally, the optical absorptance (transmittance) is proportional (inversely proportional) to optical conductivity [23]. The relatively large ρ_{xx} in FeSe thin films, measured experimentally [12], [13], [25], corresponds to a small σ_0 shown in Fig. 6(b) and a relatively short τ shown in Fig. 6(a). As a result, the optical conductivity $\sigma(\omega)$ depends relatively weakly on radiation frequency in NIR bandwidth. This becomes the main reason why NIR reflectivity from a FeSe thin film depends relatively weakly on radiation wavelength as shown in the right panel in Fig. 3. Furthermore, a small σ_0 leads to a small optical conductivity $\sigma(\omega)$. Thus, optical absorption is relatively weak in FeSe thin films due to $A(\omega) \sim \sigma_1(\omega)$. With increasing temperature, the dc resistivity ρ_{xx} increases so that the real and imaginary parts of $\sigma(\omega)$ decrease and, thus, the optical transmissivity $T_o(\omega)$ increases. Hence, the optical reflectivity $R(\omega)$ decreases with increasing temperature in FeSe thin films in metallic phase, as shown in the right panel in Fig. 3. As a consequence, the NIR reflectivity measured in the present study reflects basically the nature of conductivity in FeSe thin film samples.

4. Conclusions

In the present study, the superconducting FeSe thin films have been fabricated on CaF_2 substrates via PLD technique. We have carried out an investigation on basic optical properties of FeSe thin films via near-infrared reflection experiments. The temperature dependence of the NIR reflectivity from FeSe thin films has been examined. The main conclusions drawn from this study can be summarized as follows. i) The NIR reflection experiment can be applied to measure the superconducting transition temperature of FeSe thin films. $T_c \sim 10$ K obtained optically is in line with that measured from electric transport experiment. ii) The temperature-induced metal-to-superconductor transition in FeSe thin films can be detected optically via NIR reflectivity measurements. iii) The spectra of NIR reflectivity for FeSe can be applied for Kramers-Kronig analysis to obtain the real and imaginary parts of the optical conductivity in different temperature regimes. iv) We have found that the real and imaginary parts of the optical conductivity obtained via K-K transformation of the experimental data for reflectivity fit well with the Drude-Lorentz formula for $T \leq 100$ K and with the Drude-Smith formula for $T > 100$ K. This finding is in line with the fact that around $T_S \sim 90$ K, the FeSe thin films experience the structural phase transition. v) The NIR reflectivity measured in this study reflects basically the nature of conductivity in FeSe thin film samples. We hope that the interesting and significant experimental findings from this work can provide some important information on the physical properties, in particular the superconductivity and the phase transition, of iron-based superconductors.

References

[1] Y. Kamihara, T. Watanabe, M. Hirano, and H. Hosono, "Iron-based layered superconductor La[$O_{1-x}F_x$]FeAs (x = 0.05–0.12) with $T_c = 26$ K," *J. Amer. Chem. Soc.*, vol. 130, pp. 3296–3297, 2008.
[2] F. C. Hsu *et al.*, "Superconductivity in PbO-type structure α-FeSe," *Proc. Nat. Acad. Sci. USA*, vol. 105, pp. 14262–14264, 2008.
[3] T. Hanaguri, S. Niitaka, K. Kuroki, and H. Takagi, "Unconventional s-wave superconductivity in Fe (Se, Te)," *Science*, vol. 328, pp. 474–476, 2010.

[4] J. Paglione and R. L. Greene, "High-temperature superconductivity in iron-based materials," *Nature Phys.*, vol. 6, pp. 645–658, 2010.
[5] D. F. Liu *et al.*, "Electronic origin of high-temperature superconductivity in single-layer FeSe superconductor," *Nature Commun.*, vol. 3, 2012, Art. no. 931.
[6] J. J. Lee *et al.*, "Interfacial mode coupling as the origin of the enhancement of T_c in FeSe films on $SrTiO_3$," *Nature*, vol. 515, pp. 245–248, 2014.
[7] F. S. Li *et al.*, "Atomically resolved FeSe/$SrTiO_3$ (001) interface structure by scanning transmission electron microscopy," *2D Mater.*, vol. 3, 2016, Art. no. 024002.
[8] W. B. Qiu *et al.*, "Tuning superconductivity in FeSe thin films via magnesium doping," *ACS Appl. Mater. Interfaces*, vol. 8, pp. 7891–7896, 2016.
[9] S. Y. Zhang *et al.*, "Enhanced superconducting state in FeSe/$SrTiO_3$ by a dynamic interfacial polaron mechanism," *Phys. Rev. Lett.*, vol. 122, 2019, Art. no. 066802.
[10] W. B. Qiu *et al.*, "The interface structure of FeSe thin film on CaF_2 substrate and its influence on the superconducting performance," *ACS Appl. Mater. Interfaces*, vol. 9, pp. 37446–37453, 2017.
[11] Q. Song *et al.*, "Evidence of cooperative effect on the enhanced superconducting transition temperature at the FeSe/$SrTiO_3$ interface," *Nature Commun.*, vol. 10, 2019, Art. no. 758.
[12] B. Shen *et al.*, "Electronic structure and nematic phase transition in superconducting multiple-layer FeSe films grown by pulsed laser deposition method," *Chin. Phys. B*, vol. 26, 2017, Art. no. 077402.
[13] Z. P. Feng *et al.*, "Tunable critical temperature for superconductivity in FeSe thin films by pulsed laser deposition," *Sci. Rep.*, vol. 8, 2018, Art. no. 4039.
[14] R. H. Yuan, W. D. Kong, L. Yan, H. Ding, and N. L. Wang, "In-plane optical spectroscopy study on FeSe epitaxial thin film grown on $SrTiO_3$ substrate," *Phys. Rev. B*, vol. 87, 2013, Art. no. 144517.
[15] H. P. Wang, Z. R. Ye, Y. Zhang, and N. L. Wang, "Band structure reconstruction across nematic order in high quality FeSe single crystal as revealed by optical spectroscopy study," *Sci. Bull.*, vol. 61, pp. 1126–1131, 2016.
[16] M. Nakajima, K. Yanase, F. Nabeshima, Y. Imai, A. Maeda, and S. Tajima, "Gradual Fermi-surface modification in orbitally ordered state of FeSe revealed by optical spectroscopy," *Phys. Rev. B*, vol. 95, 2017, Art. no. 184502.
[17] M. Chinotti, A. Pal, L. Degiorgi, A. E. Böhmer, and P. C. Canfield, "Ingredients for the electronic nematic phase in FeSe revealed by its anisotropic optical response," *Phys. Rev. B*, vol. 98, 2018, Art. no. 094506.
[18] C. Zhang *et al.*, "Characterization of material parameters of $La_{0.33}Pr_{0.34}Ca_{0.33}MnO_3$ thin film by terahertz time-domain spectroscopy," *Jpn. J. Appl. Phys.*, vol. 55, 2016, Art. no. 031101.
[19] F. Pfuner, L. Degiorgi, T. I. Baturina, V. M. Vinokur, and M. R. Baklanov, "Optical properties of TiN thin films close to the superconductor-insulator transition," *New J. Phys.*, vol. 11, 2009, Art. no. 113017.
[20] C. C. Homes, Y. M. Dai, J. S. Wen, Z. J. Xu, and G. D. Gu, "$FeTe_{0.55}Se_{0.45}$: A multiband superconductor in the clean and dirty limit," *Phys. Rev. B*, vol. 91, 2015, Art. no. 144503.
[21] H. Y. Mei *et al.*, "Detection of phase separation and nano-droplet states in $La_{0.33}Pr_{0.34}Ca_{0.33}MnO_3$ nanowires via near-infrared reflection experiments," *Opt. Mater. Exp.*, vol. 7, pp. 3809–3814, 2017.
[22] D. Van Der Marel, H.-U. Habermeier, D. Heitmann, W. Kiinig, and A. Wittlin, "Infrared study of the superconducting phase transition in $YBa_2Cu_3O_{7-x}$," *Phys. C*, vol. 176, pp. 1–18, 1991.
[23] Y. M. Zhang *et al.*, "Study of spinel $LiTi_2O_4$ superconductors via near-infrared reflection experiments," *Opt. Lett.*, vol. 42, no. 8, pp. 1552–1555, 2017.
[24] H. Yang *et al.*, "Preparation and characterization of high-quality FeSe single crystal thin films," *Acta Phys. Sin.*, vol. 67, 2018, Art. no. 207416.
[25] Z. P. Feng *et al.*, "High-throughput investigation of tunable superconductivity in FeSe films," 2018, arXiv:1807.01273.
[26] Y. Imai, Y. Sawada, F. Nabeshima, D. Asami, M. Kawai, and A. Maeda, "Control of structural transition in $FeSe_{1-x}Te_x$ thin films by changing substrate materials," *Sci. Rep.*, vol. 7, 2017, Art. no. 46653.
[27] A. Maeda *et al.*, "Synthesis, characterization, hall effect and THz conductivity of epitaxial thin films of Fe chalcogenide superconductors," *Appl. Surf. Sci.*, vol. 312, pp. 43–49, 2014.
[28] W. B. Qiu *et al.*, "Enhanced superconductivity induced by several-unit-cells diffusion in an FeTe/FeSe bilayer heterostructure," *Phys. Rev. B*, vol. 99, 2019, Art. no. 064502.
[29] B. Lei *et al.*, Evolution of high-temperature superconductivity from a low-T_c phase tuned by carrier concentration in FeSe thin flakes," *Phys. Rev. Lett.*, vol. 116, 2016, Art. no. 077002.
[30] T. Passerat de Silans *et al.*, "Temperature dependence of the dielectric permittivity of CaF_2, BaF_2 and Al_2O_3: Application to the prediction of a temperature dependent van der Waals surface interaction exerted onto a neighbouring Cs($8P_{3/2}$) atom," *J. Phys., Condens. Matter*, vol. 21, 2009, Art. no. 255902.
[31] W. W. Li, H. J. Huang, B. C. Mei, J. H. Song, and X. D. Xu, "Effect of Y^{3+} ion doping on the microstructure, transmittance and thermal properties of CaF_2 transparent ceramics," *J. Alloys Compounds*, vol. 747, pp. 359–365, 2018.
[32] Y. M. Dai *et al.*, Hidden T-linear scattering rate in $Ba_{0.6}K_{0.4}Fe_2As_2$ revealed by optical spectroscopy, *Phys. Rev. Lett.*, vol. 111, 2013, Art. no. 117001.
[33] H. Lohani, P. Mishra, and B. R. Sekhar, "Investigation of correlation effects in FeSe and FeTe by LDA+U method," *Physica C*, vol. 512, pp. 54–60, 2015.
[34] C. He *et al.*, "Electronic-structure-driven magnetic and structure transitions in superconducting NaFeAs single crystals measured by angle-resolved photoemission spectroscopy," *Phys. Rev. Lett.*, vol. 105, 2010, Art. no. 117002.
[35] T. M. McQueen *et al.*, "Tetragonal-to-orthorhombic structural phase transition at 90 K in the superconductor Fe1.01Se," *Phys. Rev. Lett.*, vol. 103, 2009, Art. no. 057002.
[36] A. Charnukha, "Optical conductivity of iron-based superconductors," *J. Phys., Condens. Matter*, vol. 26, 2014, Art. no. 253203.
[37] J. Lloyd-Hughes and T.-I. Jeon, "A review of the terahertz conductivity of bulk and nano-materials," *J. Infrared, Millim. THz Waves*, vol. 33, no. 9, pp. 871–925, 2012.
[38] N. V. Smith, "Classical generalization of the Drude formula for the optical conductivity," *Phys. Rev. B*, vol. 64, no. 15, 2001, Art. no. 155106.